

Ionic conductivities of solid polymer electrolyte/salt systems for lithium secondary battery

Sung Jin Pai, Young Chan Bae*, Yang Kook Sun

Division of Chemical Engineering and Molecular Thermodynamics Laboratory, Hanyang University, Seoul 133-791, South Korea¹

Received 26 October 2004; accepted 1 February 2005

Available online 3 March 2005

Abstract

We establish a new ionic conductivity model based on the Nernst–Einstein equation in which the diffusion coefficient is derived from modified double lattice–nonrandom–Pitzer–Debye–Hückel (MDL–NR–PDH) model. The proposed model takes into account the mobility of the salt and the motion of the polymer host simultaneously by expressing the effective chemical potential as the sum of chemical potentials of the salt and the polymer. To describe the segmental motion of the polymer chain, which is the well-known conduction mechanism for solid polymer electrolyte (SPE) systems, the effective co-ordinated unit parameter is introduced. The obtained co-ordinated unit parameter for each state is used to describe the behavior of the ionic conductivities of the given systems. Good agreement is obtained upon comparison with experimental data of various PEO and salt systems in the interested ranges.

© 2005 Elsevier Ltd. All rights reserved.

Keywords: Ionic conductivity; Solid polymer electrolyte; Melting point depression

1. Introduction

Polymer-based solid electrolytes are of growing importance in solid state electrochemistry in view of their applications, the most important of which is for high-energy-density batteries. The first suggestion for the use of a poly(ethylene oxide), PEO, based electrolyte came in 1978 [1]. PEO-based complexes are thus the first solvent-free polymer electrolytes to have been reported and have received the maximum attention. Their use in lithium rechargeable batteries are now been proposed for a wide variety of extremely demanding applications [2,3].

Solid polymer electrolytes (SPEs) have improved safety for lithium battery compared to liquid electrolytes, but they are known to result with insufficient performance, especially due to low ionic conductivity. Researches on the electrochemical applications of SPEs have therefore focused on the ionic conductivity for each complex. Historically, for the quantitative study of the ionic conduction, the Vogel–

Tamman–Fulcher (VTF) equation [4] was developed independently to deal with the viscosity properties of supercooled liquids. In Armand's original publications, he stressed the temperature dependence of the conductivity, and fitted in terms of the VTF equation [1]. A parallel, but more sophisticated, set of empirical relationships in the study of the fluidity of simple hydrocarbon liquids are made by Williams, Landel and Ferry (WLF) [5]. While VTF and WLF forms of equations are very accurate for a given set of measurements, there is no guarantee that the system's behavior is governed by free-volume behavior. An especially clear formulation for free-volume theory was given by Cohen and Turnbull [6]. Since there was substantial suitability with the free-volume theory, despite its seeming complexity, many studies for the configurational entropy model were made. Adam and Gibbs [7] have analyzed WLF-type behavior in terms of configurational entropy, using only some very simplified arguments. A shortcoming of the entropy model is that like the free-volume model, it describes the motion of the polymer host in the polymer/salt complex which constitutes the solid electrolyte, but not the ionic conductivity itself [8].

Since there is more than one component in the current SPE systems, composition dependence must be taken into account in the conductivity models. Angel and Bressel [9]

* Corresponding author. Tel.: +82 2 22900520; fax: +82 2 22966280.
E-mail address: ycbae@yanyang.ac.kr (Y.C. Bae).

¹ <http://www.inchem.hanyang.ac.kr/lab/mtl/>

rationalize the composition dependence of transport properties of the bases on the VTF equation. Sørensen and Jacobsen [10] developed a simple model that accounts quantitatively for the concentration dependence of the conductivity of the low-purity-type electrolyte. Systematic studies of conductivity versus composition and temperature were made by Chabagno [11] and Fauteux et al. [12]. In view of their results, the ionic conductivity is a function of different experimental parameters and thermal history which strongly influence to a property of the amorphous phase, ion association, ion-polymer interactions, and local relaxations of the polymer. Phase characterization, especially phase diagram representation of PEO/salt systems, has appeared to be of some importance in the understanding of polymer electrolytes.

Recently, Kim and Bae [13,14] developed configurational entropy model for conductivities of SPEs that can express the composition dependence of the given systems based both on the Adam and Gibbs conductivity model and on the Flory's entropy model. To take into account the pressure effect on the ionic conductivities of the compressed SPE systems, Ahn et al. [15,16] and Choi et al. [17] extended Kim's configurational entropy model with the entropy derived from various EOSs. However, these models have the same defect resulted from the Adam and Gibbs model as mentioned above. It is important in the conductivity model for SPE systems that the salt effect must be taken into account because the ionic conduction is worked by the mobility of salt as well as the segmental motion of polymer.

The purpose of this work is to overcome the shortcomings of the previous models by taking into account the salt effect in the conductivity model. We employ the diffusion coefficient for which the driving force is based on a gradient of chemical potential. To account for the effect of both salt and polymer concurrently, the sum of each chemical potential is differentiated with concentration. Since the conduction mechanism in SPE is correlated with segmental motion of polymer chain, the effective coordination between salt and polymer units is taken into account. Each chemical potential is calculated from the phase diagram of the given system using Flory's melting point depression theory [18] combined with MDL-NR-PDH model [19]. Combination of the derived diffusion coefficient equation with Nernst-Einstein relationship yields the final conductivity equation. Comparison of the developed theory with experimental data is made for PEO and various salts systems including sodium and lithium cation.

2. Model description

2.1. MDL-NR-PDH model

In the previous work [19], we established the MDL-NR-PDH model that takes into account three different effects

explaining SPE systems: the contribution of a mixing of polymer and salt based on the modified double lattice (MDL) model [20], the nonrandomness contribution based on the expression proposed by Panayiotou et al. [21], the long-range interaction contribution using the Pitzer-Debye-Hückel expression [22]. Helmholtz free energy of mixing for the binary polymer solution is defined as the sum of the three contributions

$$\Delta A = \Delta A^{\text{MDL}} + \Delta A^{\text{NR}} + \Delta A^{\text{PDH}} \quad (1)$$

where

ΔA^{MDL} : Helmholtz energy of modified double lattice model

ΔA^{NR} : Helmholtz energy of local composition model of Panayiotou et al.

ΔA^{PDH} : Helmholtz energy of Pitzer-Debye-Hückel model

The chemical potential which is derived from differentiating Helmholtz free energy for each compound is given as follows:

The mixing contribution (MDL) [23] for salt is

$$\begin{aligned} \frac{\Delta\mu_1}{kT} = & \ln(1 - \phi_2) - r_1 \left(\frac{1}{r_2} - \frac{1}{r_1} \right) \phi_2 \\ & + r_1 \left[C_\beta \left(\frac{1}{r_2} - \frac{1}{r_1} \right)^2 + \left(\left(\frac{1}{r_2} - \frac{1}{r_1} \right) + C_\gamma \tilde{\epsilon} \right) \tilde{\epsilon} + \left(2 + \frac{1}{r_2} \right) \tilde{\epsilon} \right] \phi_2 \\ & - 2r_1 \left[\left(\left(\frac{1}{r_2} - \frac{1}{r_1} \right) + C_\gamma \tilde{\epsilon} \right) \tilde{\epsilon} + C_\gamma \tilde{\epsilon}^2 \right] \phi_2 + 3r_1 C_\gamma \tilde{\epsilon}^2 \phi_2^4 \end{aligned} \quad (2)$$

and for polymer

$$\begin{aligned} \frac{\Delta\mu_2}{kT} = & \ln \phi_2 \\ & + r_2 \left[\left(\frac{1}{r_2} - \frac{1}{r_1} \right) + C_\beta \left(\frac{1}{r_2} - \frac{1}{r_1} \right)^2 + \left(2 + \frac{1}{r_2} \right) \tilde{\epsilon} \right] \\ & - r_2 \left[\left(\frac{1}{r_2} - \frac{1}{r_1} \right) + 2 \left(\left(\frac{1}{r_2} - \frac{1}{r_1} \right) + C_\gamma \tilde{\epsilon} \right) \tilde{\epsilon} \right] \\ & + 2C_\beta \left(\frac{1}{r_2} - \frac{1}{r_1} \right)^2 + 2 \left(2 + \frac{1}{r_2} \right) \tilde{\epsilon} \right] \phi_2 \\ & + r_2 \left[4 \left(\left(\frac{1}{r_2} - \frac{1}{r_1} \right) + C_\gamma \tilde{\epsilon} \right) \tilde{\epsilon} + \left(2 + \frac{1}{r_2} \right) \tilde{\epsilon} \right] \\ & + C_\beta \left(\frac{1}{r_2} - \frac{1}{r_1} \right)^2 + 3C_\gamma \tilde{\epsilon}^2 \right] \phi_2^2 \\ & - r_2 \left[6C_\gamma \tilde{\epsilon}^2 + 2 \left(\left(\frac{1}{r_2} - \frac{1}{r_1} \right) + C_\gamma \tilde{\epsilon} \right) \tilde{\epsilon} \right] \phi_2^3 + 3r_2 C_\gamma \tilde{\epsilon}^2 \phi_2^4 \end{aligned} \quad (3)$$

where ϕ_i is the segment fraction of component i , $\phi_i = N_i r_i / N_r$, N_r ($= \sum_i N_i r_i$) is the total number of segments in the

system and r_i is the segment number of component i , 1 (salt) and 2 (polymer). C_β and C_γ are universal constants having 0.1415 and 1.7986, respectively. Reduced interaction parameter, $\tilde{\varepsilon}$, is defined by

$$\tilde{\varepsilon} = \frac{\varepsilon}{kT} - \left[\sum_i \left(\frac{\Delta A_{\text{sec},ii}}{N_{ii}kT} \right) - 2 \left(\frac{\Delta A_{\text{sec},ij}}{N_{ij}kT} \right) \right] \quad (4)$$

Helmholtz energy of mixing for the secondary lattice, $\Delta A_{\text{sec},ij}$, is given by

$$\frac{\Delta A_{\text{sec},ij}}{N_{ij}kT} = \frac{2}{z} \left[\eta \ln \eta + (1 - \eta) \ln(1 - \eta) + \frac{z C_\alpha \delta \tilde{\varepsilon}_{ij} (1 - \eta) \eta}{1 + C_\alpha \delta \tilde{\varepsilon}_{ij} (1 - \eta) \eta} \right] \quad (5)$$

where N_{ij} is the number of i - j pairs, $\delta \tilde{\varepsilon}_{ij}$ is the reduced energy parameter contributed by the oriented interactions and η is the surface fraction permitting oriented interactions and C_α is a universal constant of 0.4881.

The nonrandomness contribution (NR) is

$$\left(\frac{\Delta \mu_i}{kT} \right)_{\text{NR}} = \frac{z q_i}{2} \ln \Gamma_{ii} \quad (6)$$

where the surface factor $z q_i$ is calculated from

$$z q_i = r_i(z - 2) + 2 \quad (7)$$

For the binary solution, the nonrandomness factor between i - j pairs in Eq. (6), Γ_{ij} , is given by [21]

$$\Gamma_{12} = \frac{2}{1 + [1 - 4\theta_1\theta_2(1 - G_{12})]^{1/2}} \quad (8)$$

where θ_i is the overall surface area fraction of component i defined as $\theta_i \equiv N_i z q_i / N z q$ and the energy factor G_{12} is defined by

$$G_{ij} \equiv \exp(\alpha \Delta \delta \tilde{\varepsilon}) \quad (\Delta \delta \tilde{\varepsilon} = \delta \tilde{\varepsilon}_{11} + \delta \tilde{\varepsilon}_{22} - 2\delta \tilde{\varepsilon}_{12}) \quad (9)$$

where N_i and N represent the number of component i and the total number of molecules, respectively. As mentioned in the previous work [19], α is introduced to represent the degree of nonrandomness. Additional correlation to define the nonrandomness factor is given by

$$\Gamma_{ii} = \frac{1 - \sum_{j \neq i} \theta_j \Gamma_{ij}}{\theta_i} \quad (10)$$

where Γ_{ij} ($i \neq j$) are considered to be independent variables. Substitution of Eq. (10) into Eq. (7) corresponds to Guggenheim's molecular treatment [24].

A long-range electrostatic contribution is

$$\mu_{\pm} = \mu_{\pm}^0 + vRT \ln(\gamma_{\pm} x) \quad (11)$$

where v_i is the stoichiometric coefficient and v is defined as $v = v_+ + v_-$. From the definition, the mean activity (a_{\pm}^v) and the activity coefficient of component i (a_i) are

$$a_{\pm}^v = a_+^{v_+} a_-^{v_-}, \quad a_i = \gamma_i x_i \quad (12)$$

The expression of the activity coefficient for a solvent

(for polymer in this case) is

$$\ln \gamma_2^{\text{el}} = \frac{2A_x I_x^{3/2}}{1 + \rho^* I_x^{1/2}} \quad (13)$$

and for an ion i is

$$\ln \gamma_i^{*\text{PDH}} = -z_i^2 A_x \left[\frac{2}{\rho^*} \ln(1 + \rho^* I_x^{1/2}) + \frac{I_x^{1/2}(1 - 2I_x/z_i^2)}{1 + \rho^* I_x^{1/2}} \right] \quad (14)$$

where A_x is the usual Debye-Hückel parameter and I_x is the ionic strength given by

$$A_x = \frac{1}{3} \left(\frac{2\pi N_A \rho_s}{m_s} \right)^{1/2} \left(\frac{e^2}{\varepsilon_0 \varepsilon_s kT} \right)^{3/2}, \quad I_x = \frac{1}{2} \sum z_i^2 x_i \quad (15)$$

x_i and z_i are the mole fraction and the charge number of i component, respectively. The closest approach parameter, ρ^* , is defined by

$$\rho^* = r_0 \left(\frac{2 \times 10^6 e^2 N_A \rho_s}{m_s \varepsilon_0 \varepsilon_s kT} \right)^{1/2} = \frac{B_x}{T^{1/2}} \quad (16)$$

where

- r_0 : the hard core radius
- e : the charge of electron
- N_A : Avogadro's number
- ε_0 : the permittivity of vacuum
- ε_s : the relative permittivity of solvent
- m_s : the solvent molecular weight
- ρ_s : the solvent density

The resulting equation for γ_i of a specific ionic component i of charge z_i has one adjustable model parameter, ρ^* . Pitzer's recommendation for multi-component systems where ρ^* varies with the mole fraction, is either to take a fixed average value for ρ^* or to treat it as a fitted parameter [25].

2.2. The melting point depression theory

In a semi-crystalline system, the condition of equilibrium between a crystalline polymer and the polymer unit in the solution may be described as follows [18]

$$\mu_u^c - \mu_u^0 = \mu_u - \mu_u^0 \quad (17)$$

where μ_u^c , μ_u , and μ_u^0 are chemical potentials of crystalline polymer segment unit, liquid (amorphous) polymer segment unit and chemical potential in standard state, respectively. Now the formal difference of appearing on the left-handed side is expected as follows:

$$\mu_u^c - \mu_u^0 = -\Delta H_u (1 - T/T_m^0) \quad (18)$$

where ΔH_u is the heat of fusion per segment unit, T_m and T_m^0

are melting point temperatures of the species in a mixture and a pure phase, respectively. The right-handed side of Eq. (18) can be restated as follows:

$$\mu_u - \mu_u^0 = \frac{V_u}{V_1} \frac{r_1}{r_2} \left(\frac{\partial \Delta A}{\partial N_2} \right)_{T, V, N_1} \quad (19)$$

where V_1 and V_u are the molar volumes of the salt and of the repeating unit, respectively. By substituting Eqs. (18) and (19) into Eq. (17) and replacing T by $T_{m,2}$, the equilibrium melting temperature of mixture is given by

$$\frac{1}{T_{m,2}} - \frac{1}{T_{m,2}^0} = -\frac{k}{\Delta H_u} \frac{V_u}{V_1} \frac{r_1}{r_2} \left(\frac{\mu_2 - \mu_2^0}{kT_{m,2}} \right) \quad (20)$$

The subscripts 1, 2 and u refer to the salt, the polymer, and polymer segment unit, respectively. Similarly, we obtain for the salt (component 1)

$$\frac{1}{T_{m,1}} - \frac{1}{T_{m,1}^0} = -\frac{k}{\Delta H_1} \left(\frac{\mu_1 - \mu_1^0}{kT_{m,1}} \right) \quad (21)$$

Substituting Eqs. (3), (6) and (11)–(20) gives the equilibrium melting temperature of the polymer as

$$\begin{aligned} \frac{1}{T_{m,2}} - \frac{1}{T_{m,2}^0} = & -\frac{k}{\Delta H_u} \frac{V_u}{V_1} \frac{r_1}{r_2} \left(\ln \phi_2 + r_2 \left[\left(\frac{1}{r_2} - \frac{1}{r_1} \right) \right. \right. \\ & + C_\beta \left(\frac{1}{r_2} - \frac{1}{r_1} \right)^2 + \left. \left. \left(2 + \frac{1}{r_2} \right) \tilde{\epsilon} \right] \right. \\ & - r_2 \left[\left(\frac{1}{r_2} - \frac{1}{r_1} \right) + 2 \left(\left(\frac{1}{r_2} - \frac{1}{r_1} \right) + C_\gamma \tilde{\epsilon} \right) \tilde{\epsilon} \right. \\ & + 2C_\beta \left(\frac{1}{r_2} - \frac{1}{r_1} \right)^2 + 2 \left(2 + \frac{1}{r_2} \right) \tilde{\epsilon} \left. \right] \phi_2 \\ & + r_2 \left[4 \left(\left(\frac{1}{r_2} - \frac{1}{r_1} \right) + C_\gamma \tilde{\epsilon} \right) \tilde{\epsilon} + \left(2 + \frac{1}{r_2} \right) \tilde{\epsilon} \right. \\ & + C_\beta \left(\frac{1}{r_2} - \frac{1}{r_1} \right)^2 + 3C_\gamma \tilde{\epsilon}^2 \left. \right] \phi_2^2 \\ & - r_2 \left[6C_\gamma \tilde{\epsilon}^2 + 2 \left(\left(\frac{1}{r_2} - \frac{1}{r_1} \right) + C_\gamma \tilde{\epsilon} \right) \tilde{\epsilon} \right] \phi_2^3 \\ & + 3r_2 C_\gamma \tilde{\epsilon}^2 \phi_2^4 + \frac{zq_2}{2} \ln \Gamma_{22} + v \ln(\gamma_2^{\text{el}} x) \end{aligned} \quad (22)$$

and substituting Eqs. (2), (6) and (11) into (21) gives that of

the salt as

$$\begin{aligned} \frac{1}{T_{m,1}} - \frac{1}{T_{m,1}^0} = & -\frac{k}{\Delta H_1} \left(\ln(1 - \phi_2) - r_1 \left(\frac{1}{r_2} - \frac{1}{r_1} \right) \phi_2 c \right. \\ & + r_1 \left[C_\beta \left(\frac{1}{r_2} - \frac{1}{r_1} \right)^2 + \left(\left(\frac{1}{r_2} - \frac{1}{r_1} \right) + C_\gamma \tilde{\epsilon} \right) \tilde{\epsilon} \right. \\ & + \left. \left. \left(2 + \frac{1}{r_2} \right) \tilde{\epsilon} \right] \phi_2^2 \right. \\ & - 2r_1 \left[\left(\left(\frac{1}{r_2} - \frac{1}{r_1} \right) + C_\gamma \tilde{\epsilon} \right) \tilde{\epsilon} + C_\gamma \tilde{\epsilon}^2 \right] \phi_2 \\ & + 3r_1 C_\gamma \tilde{\epsilon}^2 \phi_2^4 + \frac{zq_1}{2} \ln \Gamma_{11} + vRT \ln(\gamma_{\pm} x) \end{aligned} \quad (23)$$

2.3. Ionic conductivity

For binary diffusion in gases or liquids, the generalized Fick's equation for heat and mass is as follows [26]:

$$\begin{aligned} J_A^* = & -cD_{AB} \left[x_A \nabla \ln a_A + \frac{1}{cRT} [(\phi_A - \omega_A) \nabla p \right. \\ & \left. - \rho \omega_A \omega_B (g_A - g_B)] + k_T \nabla \ln T \right] \end{aligned} \quad (24)$$

This equation represents that the thermodynamics of irreversible processes dictates using the activity gradient as the driving force for concentration diffusion. This requires a diffusion coefficient different from Fick's first law. When the pressure-, thermal-, and forced-diffusion terms are dropped, Eq. (24) for binary electrolyte is simplified by

$$J_s^* = -D^* C_s \nabla \ln a_s \quad (25)$$

where D^* , C_s and a_s are self-diffusion coefficient, concentration and activity of salt, respectively. This may be rewritten by making use of the fact that the activity is a function of concentration to obtain

$$J_s^* = -D^* C_s \left(\frac{d \ln a_s}{d C_s} \right) \nabla C_s \quad (26)$$

When comparing Eq. (26) with the original Fick's equation, $J_s^* = -D_s \nabla C_s$, this is related to the measured diffusion coefficient D_s (based on a concentration driving force) by [26]

$$D_s = D^* \left(\frac{d \ln a_s}{d \ln c_s} \right) \quad (27)$$

where D^* characterizes the component mobility in the

absence of any interactions in the given system [27]. This may be rewritten by the fact that the activity is related to the chemical potential by $\ln a = \Delta\mu/RT$

$$D_s = D^* C_s \frac{d\left(\frac{\Delta\mu_s}{RT}\right)}{dC_s} \quad (28)$$

The transport of cations in solvent-free polymer electrolytes differs from that of systems based on molecular liquids or low molar mass polymers. In the latter systems, ions can move together with their co-ordinated solvent, but in the case of high molecular weight polymers the centre of gravity of the chain cannot be moved significant distances. For electrolytes using high molecular weight polymers, cation transport does not only occur in conjunction with polymer diffusion but lithium ion transport also occurs as a result of segmental motion [28]. Since cations move across co-ordinating sites which are made up of the acid–base interactions between solvent and solute molecules, diffusion of cation must be taken into account with effective co-ordinated polymer units. To express this co-ordinating effect in the conductivity model, the chemical potential in Eq. (28) is replaced by the sum of chemical potentials of salt and effective co-ordinating polymer units, which is given by

$$D_s = D^* C_s \frac{d\left(\frac{\Delta\mu_{\text{eff}}}{RT}\right)}{dC_s}, \quad \frac{\Delta\mu_{\text{eff}}}{RT} = \frac{\Delta\mu_s}{RT} + \lambda_{\text{eff}} \frac{\Delta\mu_u}{RT} \quad (29)$$

where λ_{eff} is the effective co-ordinated units of polymer. A mathematical form of $\lambda_0 e^{\omega C_s}$ is adopted for λ_{eff} based on the exponentially lowering coordinating units, where λ_0 and ω are adjustable model parameters, respectively.

This in turn yields, using the Nernst–Einstein relationship for multi-component system, the conductivity equation

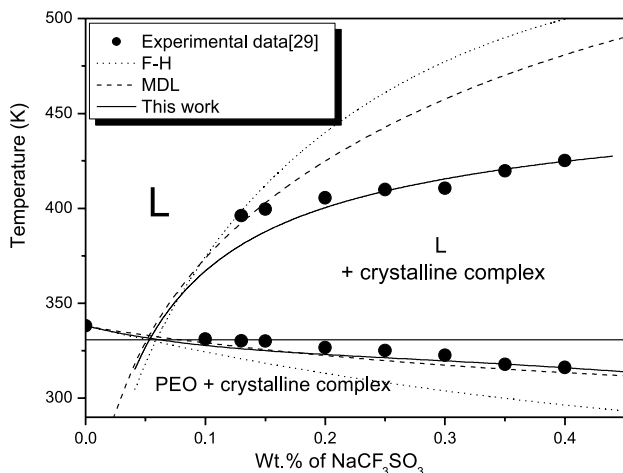


Fig. 1. Phase diagram for the PEO/NaCF₃SO₃ system. The dark circles are experimental melting point data reported by Pai et al. [29]. The solid lines are calculated by the proposed model, the dashed lines by the MDL model and the dotted line by the Flory–Huggins theory.

for SPE having the form as:

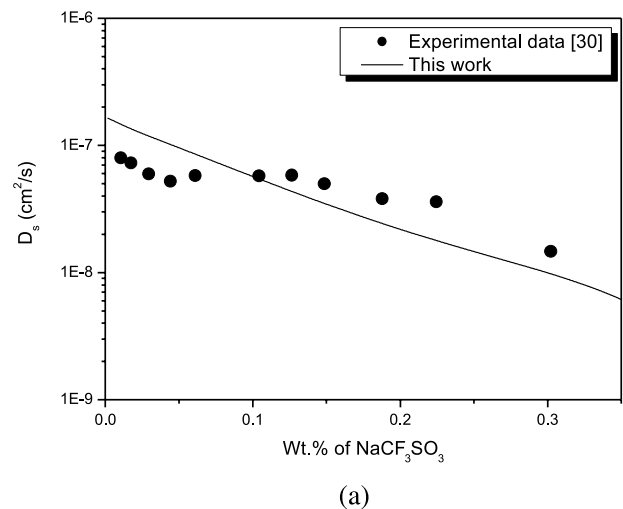
$$\sigma = \frac{F^2}{RT} \sum_i z_i^2 v_i D_i C_i \quad (30)$$

where F is a Faraday constant. Since we assume that the phase at the given condition is binary system of polymer and salt, the moving object is salt itself instead of cation. If the charge effect of each ion remains for the ion interactions, this assumption makes Eq. (30) a simple form

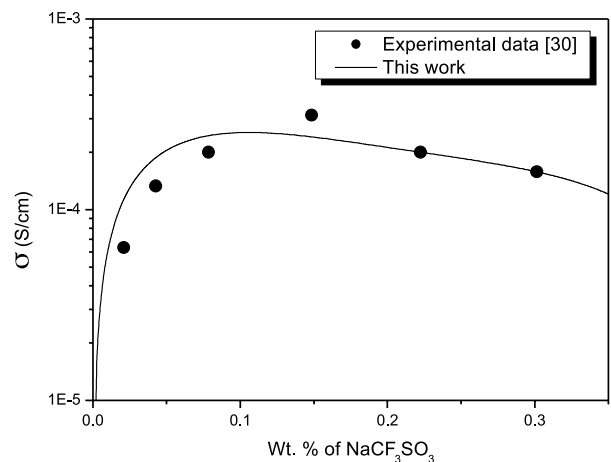
$$\sigma = \frac{F^2 C_s}{RT} D_s \sum_i z_i^2 \quad (31)$$

Substituting Eq. (29) into Eq. (31) gives the final ionic conductivity equation for SPE systems

$$\sigma = \frac{F^2 C_s}{RT} D^* C_s \frac{d\left(\frac{\Delta\mu_s}{RT} + \lambda_0 e^{\omega C_s} \frac{\Delta\mu_u}{RT}\right)}{dC_s} \sum_i z_i^2 \quad (32)$$



(a)



(b)

Fig. 2. Transport properties of PEO/NaCF₃SO₃ system: (a) Diffusion coefficient, (b) ionic conductivity at 358.15 K. The dark circles are experimental data reported by Yanping et al. [30], and the lines are calculated values using the proposed model.

Table 1
Physical properties of PEO and salts

	T_m^0 (K)	ΔH (J mol ⁻¹)	MW (g mol ⁻¹)	Density (g cm ⁻³)	V_u (cm ³ mol ⁻¹)
PEO	338.15	6798.00 ^a	5,000,000	1.21	36.6
	338.15	8284.32 ^a	900,000	1.21	36.6
NaCF ₃ SO ₃	527.15	10433.72	172.06	1.13	36.0
LiClO ₄	509.15	14600.00	106.39	2.43	43.8
LiAsF ₆	525.63	57188.20	195.85	2.65	73.91

^a J unit⁻¹.

where the chemical potentials are given by

$$\begin{aligned} \frac{\Delta\mu_s}{RT} = & \ln(1 - \phi_2) - r_1 \left(\frac{1}{r_2} - \frac{1}{r_1} \right) \phi_2 \\ & + r_1 \left[C_\beta \left(\frac{1}{r_2} - \frac{1}{r_1} \right)^2 + \left(\left(\frac{1}{r_2} - \frac{1}{r_1} \right) + C_\gamma \tilde{\varepsilon} \right) \tilde{\varepsilon} \right. \\ & + \left. \left(2 + \frac{1}{r_2} \right) \tilde{\varepsilon} \right] \phi_2^2 \\ & - 2r_1 \left[\left(\left(\frac{1}{r_2} - \frac{1}{r_1} \right) + C_\gamma \tilde{\varepsilon} \right) \tilde{\varepsilon} + C_\gamma \tilde{\varepsilon}^2 \right] \phi_2 \\ & + 3r_1 C_\gamma \tilde{\varepsilon}^2 \phi_2^4 + \frac{zq_1}{2} \ln \Gamma_{11} + vRT \ln(\gamma_s x) \end{aligned} \quad (33)$$

and

$$\begin{aligned} \frac{\Delta\mu_u}{RT} = & \frac{V_u}{V_1} \\ & \times \frac{r_1}{r_2} \left(\ln \phi_2 + r_2 \left[\left(\frac{1}{r_2} - \frac{1}{r_1} \right) + C_\beta \left(\frac{1}{r_2} - \frac{1}{r_1} \right)^2 \right. \right. \\ & + \left. \left. \left(2 + \frac{1}{r_2} \right) \tilde{\varepsilon} \right] \right) \\ & - r_2 \left[\left(\frac{1}{r_2} - \frac{1}{r_1} \right) + 2 \left(\left(\frac{1}{r_2} - \frac{1}{r_1} \right) + C_\gamma \tilde{\varepsilon} \right) \tilde{\varepsilon} \right. \\ & + \left. 2C_\beta \left(\frac{1}{r_2} - \frac{1}{r_1} \right)^2 + 2 \left(2 + \frac{1}{r_2} \right) \tilde{\varepsilon} \right] \phi_2 \\ & + r_2 \left[4 \left(\left(\frac{1}{r_2} - \frac{1}{r_1} \right) + C_\gamma \tilde{\varepsilon} \right) \tilde{\varepsilon} + \left(2 + \frac{1}{r_2} \right) \tilde{\varepsilon} \right. \\ & + \left. C_\beta \left(\frac{1}{r_2} - \frac{1}{r_1} \right)^2 + 3C_\gamma \tilde{\varepsilon}^2 \right] \phi_2 \\ & - r_2 \left[6C_\gamma \tilde{\varepsilon}^2 + 2 \left(\left(\frac{1}{r_2} - \frac{1}{r_1} \right) + C_\gamma \tilde{\varepsilon} \right) \tilde{\varepsilon} \right] \phi_2 \\ & + 3r_2 C_\gamma \tilde{\varepsilon}^2 \phi_2 + \frac{zq_2}{2} \ln \Gamma_{22} + v \ln(\gamma_2^{\text{el}} x) \end{aligned} \quad (34)$$

3. Results and discussion

Fig. 1 shows the phase diagram of PEO ($M_w = 5,000,000$ g mol⁻¹)/NaCF₃SO₃ system. Dark circles are experimental data reported by Pai et al. [29] and solid lines are calculated by the MDL-NR-PDH model. The polymer (lower solid line) and crystalline complex (upper solid line) melting curves are calculated from Eqs. (22) and (23), respectively. We let the number of the salt segment, r_1 , be a unity and calculate the number of the polymer units, r_2 , using specific volumes V_1 and V_2 for solvent and polymer,

$$r_2 = \frac{M_2 V_2}{M_1 V_1} \quad (35)$$

where M_1 and M_2 are molecular masses for salt and polymer, respectively. We set $\eta = 0.3$ and $z = 6$ as suggested by Hu et al. [27] and set the nonrandomness parameter, α , 0.03 [19].

Table 1 gives physical properties of PEO and salts and the model parameters are listed in Table 2. The estimated eutectic point at the intersection of the two curves is wt% of salt ≈ 0.05 . Dashed and dotted lines are calculated from the MDL model [20] and Flory–Huggins (F–H) theory [18], respectively. As seen in the figure, the present work (solid line) describes the experimental data very well compared to those of other models.

Fig. 2 shows transport properties of PEO/NaCF₃SO₃ system. The dark circles are experimental data reported by Yanping et al. [30] and the lines are calculated by the proposed model. To differentiate chemical potential with concentration, the salt concentration is calculated from the salt mass fraction as follows:

$$C_1 = \frac{\rho_1 w_1}{M_1} \quad (36)$$

Table 2
Chemical potential parameters for PEO/salt system

	ε/k (K)	$\delta\varepsilon_{12}/k$ (K)	B_x (K ^{1/2})
PEO/NaCF ₃ SO ₃	-102.730	2,080.172	22,510.160
PEO/LiClO ₄ (wt% 0.2–0.29)	1,366.780	-1,419.710	5,183.140
PEO/LiClO ₄ (wt% 0.29–)	1,157.231	-1,547.080	52,750.057
PEO/LiAsF ₆	1,325.359	-1,776.722	3,024.513

Table 3
Diffusion and co-ordinated unit parameters for PEO/salt systems

		D^* (cm ² s ⁻¹)	λ_0 (-)	ω (cm ³ mol ⁻¹)
PEO/NaCF ₃ SO ₃		1.596×10^{-7}	1.254	-14.354
PEO/LiClO ₄	338 K	7.475×10^{-8}	6.602	53.835
	358 K	2.932×10^{-7}	14.750	-261.319
	378 K	5.525×10^{-7}	12.491	-229.923
	398 K	8.171×10^{-7}	9.686	-184.65
PEO/LiAsF ₆	338 K	1.165×10^{-7}	24.839	-437.761
	358 K	4.818×10^{-7}	24.613	-435.052
	378 K	1.322×10^{-6}	21.909	-392.936
	398 K	2.670×10^{-6}	17.988	-324.014

where w_1 is the weight fraction of salt. The density of salt, ρ_1 , is given by

$$\frac{1}{\rho_1} = \frac{1}{\rho_2^0} + w_1 \left(\frac{V_1}{M_1} - \frac{1}{\rho_2^0} \right) \quad (37)$$

where ρ_2^0 is the density of pure PEO. In Fig. 2(a), the measured diffusion coefficients are fitted using Eq. (29).

Model parameters are determined and listed in Table 3. In this case, the co-ordinated unit parameter, λ_{eff} , is nearly a unity, meaning that, at the given temperature, the PEO/NaCF₃SO₃ system has nearly one-to-one bonding between the salt and the polymer unit. Using Eq. (32) with previously determined model parameters, the ionic conductivity of the given system is calculated as a function of salt

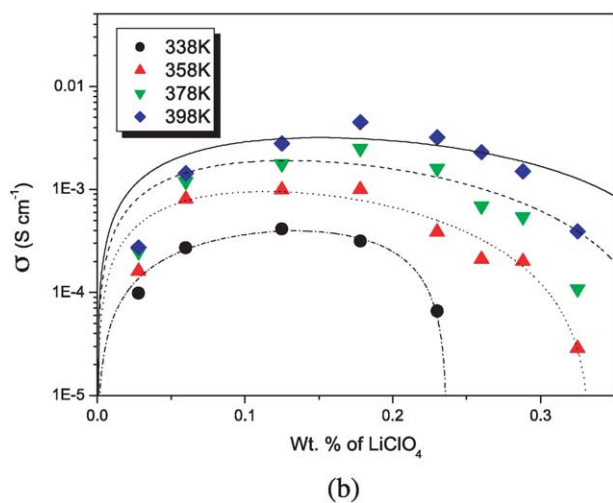
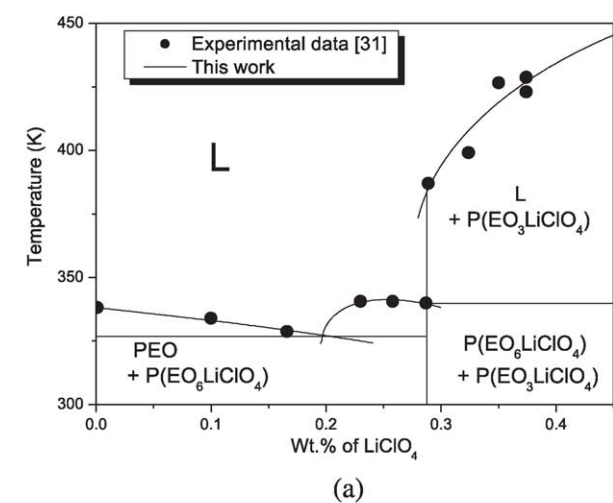


Fig. 3. (a) Phase diagram and (b) ionic conductivity of PEO/LiClO₄ system. Experimental data are reported by Robitaille et al. [31]. Lines are calculated by the proposed model.

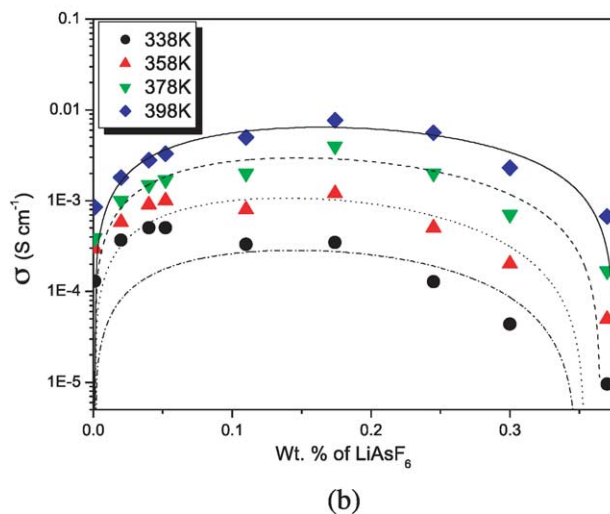
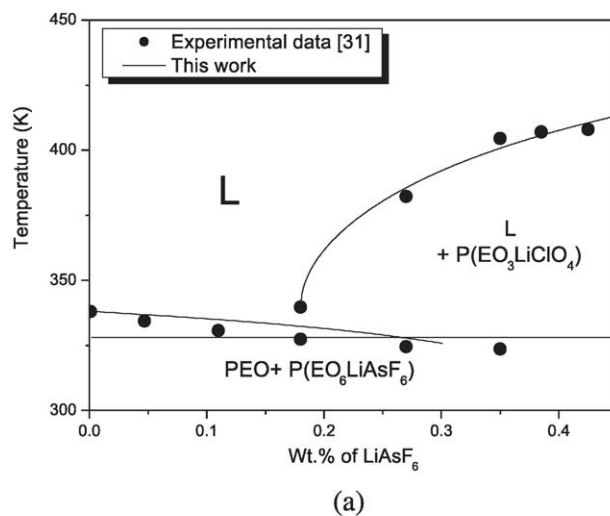


Fig. 4. (a) Phase diagram and (b) ionic conductivity of PEO/LiAsF₆ system. Experimental data are reported by Robitaille et al. [31] and the lines are calculated by the proposed model.

weight fraction. As can be seen in Fig. 2(b), calculated values agree fairly well with experimental data.

Fig. 3 shows the phase diagram and the ionic conductivity of PEO/LiClO₄ system. Dark circles are experimental data reported by Robitallie et al. [31] and the lines are calculated by the proposed model. There is a leap point in the crystalline complex melting curve at wt% of salt ≈ 0.29 . As shown in Table 2, the energy parameter values, ε/k and $\delta\varepsilon_{12}/k$, are similar for two different salt wt% region. The closest approach parameters, B_x , however, differ by one order, meaning that the lower salt concentration part is more closely packed than those of higher salt concentration region. By using these parameters the ionic conductivity was fitted for each isothermal data to give the diffusion and co-ordinated unit parameters (Fig. 3(b)). At 338 K, the fitted values agree well with the experimental data, but there are some deviations in dilute region.

Fig. 4 shows the phase diagram and the ionic conductivity for PEO/LiAsF₆ system, in which the experimental data are reported by Robitallie et al. [31]. In Fig. 4(a), the proposed model agrees well with the experimental data in the entire region and the estimated eutectic point is wt% of salt ≈ 0.18 . In Fig. 4(b), the proposed model agrees well fairly with the ionic conductivity data in the entire region. The decrease at wt% of salt ≈ 0.1 may represent the change of the phase. In this case, the electrolyte instability makes it impossible to define the variation of the ionic conductivity for wt% of salt > 0.35 properly [31].

4. Conclusion

We introduced two ideas in the ionic conductivity model: one is the concentration dependence of the diffusion coefficient expressed by differentiating chemical potential with concentration and the other is the polymer segmental motion by introducing the effective co-ordinated unit parameters. The former relates the phase behavior of the given system to the diffusion and the ionic conductivity, and the latter explains why the ionic conductivity decreases sharply beyond certain wt%. The calculated values using the proposed model agree well with the experimental data for systems of PEO/ sodium or lithium salts.

Acknowledgements

This work is supported in part by the Ministry of

Information & Communication of Korea ('Support Project of University Information Technology Research Center' supervised by IITA).

References

- [1] Armand MB, Chabagno JM, Duclot M. Second international meeting on solid electrolytes, St Andrews, Scotland; September 20–22, 1978. Extended Abstract.
- [2] Hooper A, North JM. Solid state ionics, 9 and 10 1983. p. 1161.
- [3] Gauthier M, Fauteux D, Vassort G, Bélanger A, Duval M, Ricoux P, et al. Second international meeting on lithium batteries, Paris, France; April 25–27, 1984.
- [4] Vogel H. Phys Z 1921;22:645. Tamman G, Hesse W, Anorg Z. Z Anorg Allg Chem 1926;156:245. Fulcher GS. J Am Ceram Soc 1925; 8:339.
- [5] Williams ML, Landel RF, Ferry JD. J Am Chem Soc 1955;77:3704.
- [6] Cohen MH, Turnbull D. J Chem Phys 1959;31:1164.
- [7] Adam G, Gibbs JH. J Chem Phys 1965;43:139.
- [8] MacCallum JR, Vincent CA. Polymer electrolyte reviews. Amsterdam: Elsevier; 1987. p. 201.
- [9] Angel CA, Bressel RD. J Phys Chem 1972;76:3244.
- [10] Sørensen PR, Jacobsen T. Polym Bull 1983;9:47.
- [11] Chabagno JM. Thesis, Institut National Polytechnique, Grenoble; 1980.
- [12] Fauteux D, Robitaille C. J Electrochem Soc 1986;133:307.
- [13] Kim JY, Bae YC. J Appl Polym Sci 1999;73:1891.
- [14] Kim JY, Bae YC. Fluid Phase Equilib 1999;163:291.
- [15] Ahn WY, Bae YC. J Polym Sci: Part B: Polym Phys 2001;39:1484.
- [16] Ahn WY, Bae YC. J Polym Sci: Part B: Polym Phys 2002;40:706.
- [17] Choi YS, Bae YC. Polymer 2003;44:3753.
- [18] Flory PJ.. 8th ed Principles of polymer chemistry. Ithaca: Cornell University Press; 1971. p. 568.
- [19] Pai SJ, Bae YC. Fluid Phase Equil. In press.
- [20] Oh JS, C Y. Bae. Polymer 1998;39(5):1149.
- [21] Panayiotou C, Vera JH. Fluid Phase Equilib 1980;5:55.
- [22] Pitzer KS. J Phys Chem 1973;77:268.
- [23] Hu Y, Lambert SM, Soane DS, Prausnitz JM. Macromolecules 1991; 24:4356.
- [24] Guggenheim EA. Mixtures. Oxford: Clarendon Press; 1952.
- [25] Tester JW, Modell M. 3rd ed. Thermodynamics and it's applications. New Jersey: Prentice Hall; 1997. p. 535.
- [26] Bird RB, Stewart WE, Lightfoot EN. Transport phenomena. 2nd ed. New York: Wiley; 2002. p. 770.
- [27] Zaikov GE, Iordanskii AL, Markin VS. Diffusion of electrolytes in polymers.: VSP BV; 1988. p. 9.
- [28] Gray FM. Polymer electrolytes.: The Royal Society of Chemistry; 1997. p. 104.
- [29] Pai SJ, Bae YC. J Electrochem Soc. 2005;152(5).
- [30] Ma Y, Doyle M, Fuller TF, Doeff MM, DeJonghe LC, Newman J. J Electrochem Soc 1995;142:1859.
- [31] Robitallie CD, Fauteux D. J Electrochem Soc 1986;133:315.